Cloning and characterization of maxi K^+ channel α-subunit in rabbit kidney

TAKASHI MORITA,[1] KAZUSHIGE HANAOKA,[1] MARCELO M. MORALES,[1] CHAHRZAD MONTROSE-RAFIZADEH,[2] AND WILLIAM B. GUGGINO[1]
[1]*Department of Physiology, Johns Hopkins University School of Medicine, and* [2]*National Institute on Aging, Baltimore, Maryland 21205*

Morita, Takashi, Kazushige Hanaoka, Marcelo M. Morales, Chahrzad Montrose-Rafizadeh, and William B. Guggino. Cloning and characterization of maxi K^+ channel α-subunit in rabbit kidney. *Am. J. Physiol.* 273 (*Renal Physiol.* 42): F615–F624, 1997.—We have identified in rabbit renal cells two alternatively spliced transcripts of the α-subunit *rbslo1* and *rbslo2*. *Rbslo1* has a novel "in-frame" 174-bp insertion immediately after the predicted S8 transmembrane segment, whereas *rbslo2* has a 104-bp deletion between S9 and S10, creating a frameshift and a premature termination codon. Amino acid identity between mouse maxi K^+ channel α-subunit (*mslo*) and *rbslo1* was 99%. Two transcript sizes of 4.2 and 7.5 kb were detected in brain, kidney, stomach, testis, and lung. *Rbslo* is expressed in glomeruli, thin limbs of Henle's loop, medullary and cortical thick ascending limbs of Henle's loop, and cortical, outer, and inner medullary collecting ducts; however, it was rarely detected in proximal convoluted tubules. *Rbslo1* is most abundant in inner medulla. Expressed in *Xenopus* oocytes, *rbslo1* generates depolarization-activated, outwardly rectifying K^+ currents. *Rbslo1* expressed in Chinese hamster ovary cells could be activated by depolarization and Ca^{2+}. These data suggest that *rbslo* transcripts are expressed in multiple nephron segments and that the magnitude of mRNA expression varies among different nephron segments.

potassium channels; cloning; calcium; potassium transport

LARGE CONDUCTANCE (maxi) Ca^{2+}-activated K^+ channels are expressed in several nephron segments (10, 15, 20, 21, 23, 24). Although the exact function of these channels in most renal epithelia is unclear, they provide cells with a pathway for large movements of K^+. For example, Ca^{2+}-activated K^+ channels are activated during hypotonic stress in cultured medullary thick ascending limb (MTAL) cells via an increase of intracellular Ca^{2+} concentration ($[Ca^{2+}]_i$) (3, 22, 28). The increase in $[Ca^{2+}]_i$ is through a dihydropyridine-sensitive Ca^{2+} influx mechanism (17, 22). The activation of Ca^{2+}-activated K^+ channels following hypotonic stress provides cells with a mechanism to quickly lose K^+ during regulatory volume decrease (22, 23, 25, 28).

Because of the relatively high concentrations of Ca^{2+} required to activate the channels, they probably are not active under basal conditions. However, the modulation of maxi K^+ channel activity by protein kinase A, protein kinase G, and inhibition of dephosphorylation is well documented in other tissues (2, 13, 29), suggesting that phosphorylation of channel protein is important in regulating channel activity. We have shown in cultured kidney cells that forskolin and antidiuretic hormone can activate Ca^{2+}-activated K^+ channels, probably via phosphorylation of the channel protein (9). This suggests that, under some stimulated conditions, Ca^{2+}-activated K^+ channels may indeed play a role in transcellular transport.

Two subunits of maxi K^+ channel have been cloned (5, 11). The α-subunit is the functional unit which is inhibited by iberiotoxin (IBTX). The β-subunit does not produce any current when it is expressed in *Xenopus* oocytes. However, coexpression of the α- and β-subunits in *Xenopus* oocytes produces currents with increased Ca^{2+} and voltage sensitivity, compared with the current produced by expression of α-subunit alone (19).

Although several groups using electrophysiological techniques have shown that maxi K^+ channels exist in several nephron segments (10, 15, 20, 21, 24), the distribution and the abundance of these channels in each cell type at molecular level have not been reported. To evaluate these channels at the molecular level, we have cloned the rabbit maxi K^+ channel α-subunit from MTAL cells using polymerase chain reaction (PCR) cloning strategy based on the amino acid sequences of *Drosophila* and mouse brain maxi K^+ channels and examined the tissue distribution of the mRNA in rabbit kidney.

MATERIAL AND METHODS

Reverse transcriptase (RT)-PCR analysis. Total RNA was prepared from rabbit MTAL cells (3). cDNA was synthesized from 1 μg of total RNA using Superscript Reverse Transcriptase (Life Technologies), according to the manufacturer's instructions. PCR amplification was performed with degenerate primers, based on the published sequences of *dslo* and *mslo* (1, 5), sense primer (5′ GTIACCATGTCCACIGTIG 3′) and antisense primer [5′ CAIGACTGGGCGAT(G/A)AAIC 3′] with 40 cycles of denaturation (94°C, 1 min), annealing (50°C, 1 min), and extension (72°C, 1 min). The PCR product was ligated into PCRscript (Stratagene) according to the manufacturer's instructions and sequenced using the Sequenase 2.0 kit (Amersham).

To study the expression of alternatively spliced isoforms of *rbslo*, PCR primers were selected from either the additional exon or regions flanking the deleted exons (Fig. 1). Total RNA was isolated from various tissues. One microgram of each total RNA was treated with deoxyribonuclease I (1 U/μl) at 37°C for 15 min and inactivated at 94°C for 15 min. cDNA was synthesized as described above and amplified with the sense primer (5′ GTTACGGGGACGTTTATGC 3′) and antisense primer (5′ CCAACTTCAGCTCTGCAAG 3′) with 35 cycles of denaturation (94°C, 1 min), annealing (58°C, 1 min), and extension (72°C, 1 min). PCR amplification of the A spliced site was performed using a specific sense primer (5′ CAAGATGTCCATCTACAAG 3′) and an antisense primer (5′ GGAAACGGGTGCAGCAATC 3′) with 40 cycles of denaturing (94°C, 1

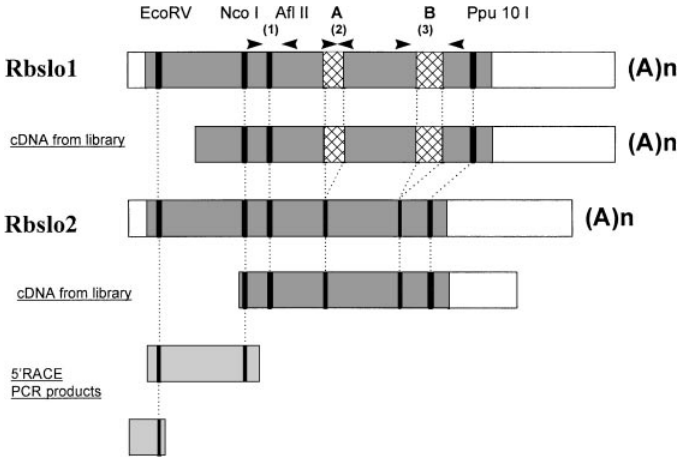

Fig. 1. Schematic presentation of clones of *rbslo*. Total length of *rbslo1* cDNA from overlapping fragments is 4,114 bp. Method used to get each fragment is underlined (*left*). Sites of restriction enzymes used to make composite clones are indicated by bold lines. Inserted or deleted exons at splice junction sites are depicted by cross hatches. (A)n, polyadenylation tails. Sites of primers used in Fig. 4 are indicated by arrows and designated in parentheses (*top*) 5′ RACE, 5′ rapid amplification of cDNA ends; PCR, polymerase chain reaction.

min), annealing (55°C, 1 min), and extension (72°C, 1 min). The B spliced site was amplified with the sense strand primer (5′ GTGCCAGCAACTTCCATTAC 3′) and antisense primer (5′ GGAGAGGATCTGTCCATTC 3′) with 40 cycles of denaturation (94°C, 1 min), annealing (57°C, 1 min), and extension (72°C, 1 min) (Fig. 4).

Products were electrophoresed on 1% agarose gels and blotted onto nylon membranes (Hybond N^+, Amersham). ^{32}P random-labeled probes of the amplified *rbslo* regions or ^{32}P 5′ end-labeled PCR primers were hybridized in QuikHybe (Stratagene) and washed in 40 mM Na_2HPO_4 (pH 7.2) at room temperature and then in 40 mM Na_2HPO_4 with 5% sodium dodecyl sulfate (SDS) (pH 7.2) at 65°C for 20 min. The blot was wrapped in Saran Wrap (Dow Brands) and exposed to autoradiography film at −80°C.

Library screening and cDNA sequencing. A cDNA library was constructed in λZAP (Stratagene) using size-fractionated mRNA from MTAL cells, based on work previously done (16). The cDNA library was screened with a ^{32}P 5′ end-labeled oligonucleotide probe (5′ GTGACCATGAGCACTGTTGGTTACGGGGACGTTTATGC 3′) hybridized in 6× standard sodium citrate (SSC), 1× Denhardt's solution, 0.05% sodium pyrophosphate, and 100 μg/ml yeast tRNA at 42°C overnight after prehybridization in 6× SSC, 5× Denhardt's solution, 0.05% sodium pyrophosphate, 0.5% SDS, and 100 μg/ml salmon sperm DNA at 42°C for 3 h. The filters were washed once in 2× SSC, 0.1% SDS at room temperature and once in 0.1× SSC, 0.1% SDS at 52°C.

Bacteriophage clones were excised in vivo to pBluescript following the manufacturer's protocol. Nested deletions of the pBluescript clones were constructed using the *Exo* III/Mung Bean Nuclease Deletion Kit (Stratagene), according to the manufacturer's instructions. The nested deletion clones were sequenced with the Sequenase 2.0 kit (Amersham).

5′ Rapid amplification of cDNA ends PCR. Single-stranded cDNAs were synthesized using either of the antisense primers (5′ GACACATTCCCAGTACGTG 3′ or 5′ GTTGGACGAATCTATGAAG 3′). An anchor oligonucleotide (5′ CCTCTGAAGGTTCCAGAATCGATAG 3′) was ligated to the single-stranded cDNAs using T4 RNA ligase and then amplified using either a combination of Klentaq (Ab Peptides) and *Pfu* polymerase (Stratagene) or *Pfu* polymerase alone. The PCR products were cloned and sequenced, as described above, and subcloned into clones from the cDNA library using unique restriction sites (*Nco* I, *Eco*R V; Fig. 1).

Northern blotting. Polyadenylated mRNA was prepared from various tissues. Two micrograms of poly(A)$^+$ mRNA were electrophoresed on a formamide-formaldehyde denaturing agarose gel and blotted onto a nylon membrane (Hybond N^+, Amersham). The *rbslo* cDNA was random labeled with [α-^{32}P]dCTP (NEN, 3,000 mCi/mmol) and used as a probe. Blots were hybridized overnight at 65°C in 0.5 M Na_2HPO_4 (pH 7.2), 7% SDS, 2 mM EDTA, and 100 μg/ml salmon sperm DNA, washed twice with 40 mM Na_2HPO_4, 5% SDS at the same temperature, and then autoradiographed.

RT-PCR analysis of microdissected nephron segments. Microdissection of nephron segments and reverse transcription of mRNA were performed as previously described with minor modifications (31). In brief, 1 mm of each nephron segment was microdissected and permeabilized. cDNA was synthesized with a specific primer (5′ CAGGACTGGGCGATGAAAC 3′). PCR amplification consisted of two nested rounds. The first round was performed with a sense primer (5′ GTTACGGGGACGTTTATGC 3′) and antisense primer (5′ CAGGACTGGGCGATGAAC 3′) with 40 cycles of denaturation (94°C, 1 min), annealing (56°C, 1 min), and extension (72°C, 1 min). One-tenth of the first-round product was amplified using the sense primer (5′ GTTACGGGGACGTTTATGC 3′) and antisense primer (5′ CCAACTTCAGCTCTGCAAG 3′) with 40 cycles of denaturation (94°C, 1 min), annealing (58°C, 1 min), and extension (72°C, 1 min).

Ribonuclease protection assay (RPA). The PCR product corresponding to *rbslo* nucleotide sequences 2599 through 2797 was subcloned into PCRscript SK(+). Riboprobe was prepared from linearized plasmid by in vitro transcription (Ambion) and incorporated [α-^{32}P]UTP (NEN, 800 mCi/mmol). Total RNA samples were prepared from resected kidneys using the cesium chloride ultracentrifugation method. Total RNA (40 μg) was hybridized with the labeled riboprobe (1×10^5 counts/min) for 24 h. The samples were digested with a mixture a ribonuclease A and ribonuclease T1 (Ambion), then analyzed on an 8 M urea-5% polyacrylamide gel, and autoradiographed. The exposed film was analyzed using ImageQuant software (Molecular Dynamics). An internal control of 18S ribosomal RNA was also quantified using RPA ($pT_7$18S, Ambion).

Expression in Xenopus oocytes. The composite cDNA clones were constructed in pBluescript SK(+), linealized, and in vitro transcribed to capped cRNA using T7 RNA polymerase. The cRNA was diluted to 50 ng/μl in diethyl pyrocarbonate-treated water, and 50 nl of the individual cRNA were injected into *Xenopus* oocytes prepared as described previously (16). The detail protocol for oocyte current recording was followed as previously described (16). In brief, two electrode voltage-clamp recordings were performed in ND96 solution [96 mM NaCl, 2 mM KCl, 1 mM $CaCl_2$, 1 mM $MgCl^2$, and 5 mM *N*-2-hydroxyethylpiperazine-*N*′-2-ethanesulfonic acid (HEPES), pH 7.4]. Niflumic acid (150 μM) was always added into the bath solution to prevent endogenous Ca^{2+}-activated Cl^- current. Command protocols were generated, and currents were acquired by using an Axoclamp-2A amplifier (Axon Instruments) interfaced to a IBM-AT-compatible 486 microcomputer (Gateway 2000) via pCLAMP version 6.02 software (Axon Instruments).

To determine ion selectivity of the expressed currents, the following protocol was used. The solutions used were 76 mM NaCl, 20 mM *X*Cl (*X* = Na, K, Rb, or NH_4), 1 mM $CaCl_2$, 1 mM $MgCl_2$, and 5 mM HEPES (pH 7.4), and they were serially

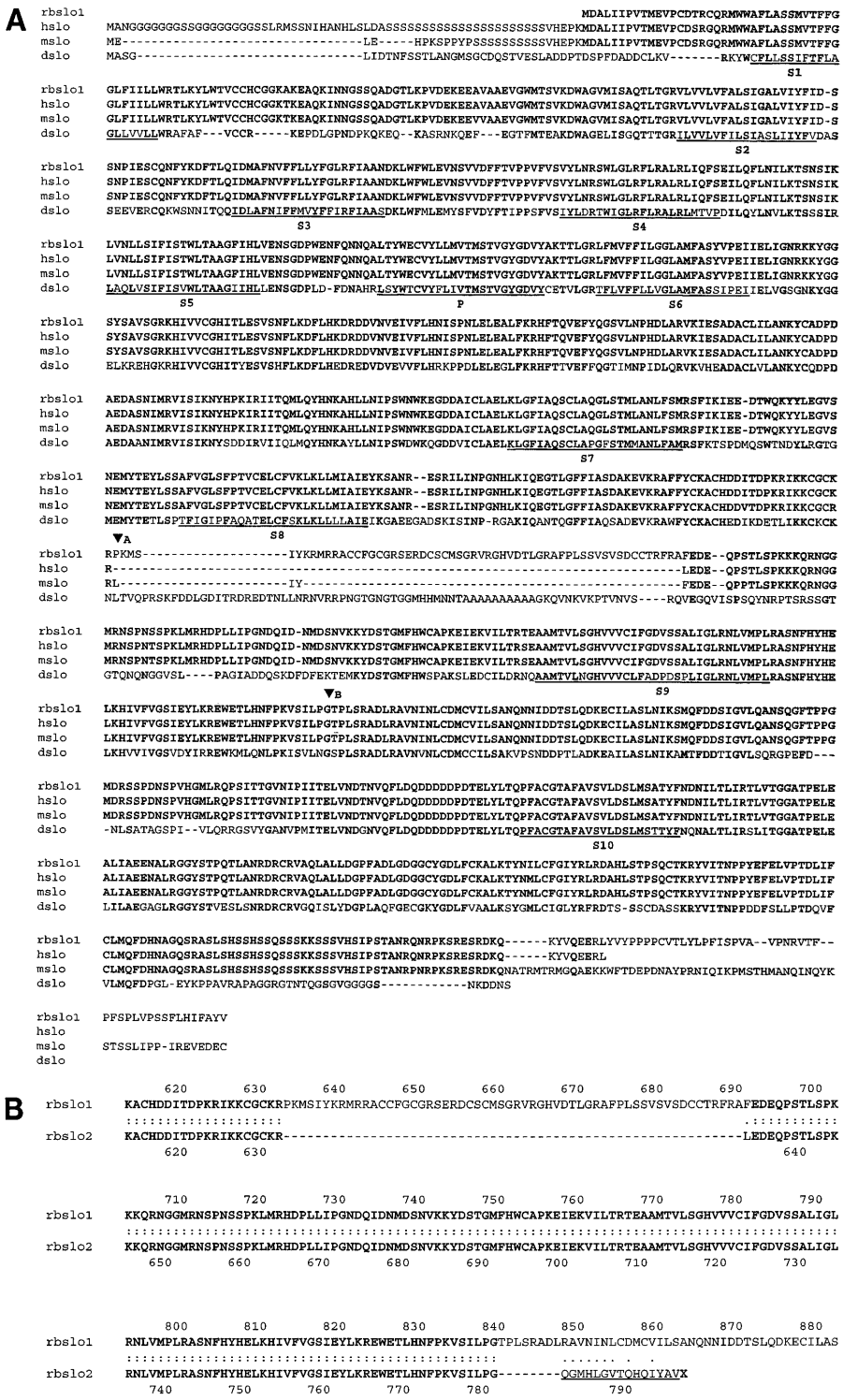

Fig. 2. Alignment of maxi K^+ channel α-subunit cDNA clones. *A*: deduced amino acid sequence of *rbslo1* is aligned with those of human maxi K^+ channel α-subunit (*hslo*), mouse maxi K^+ channel α-subunit (*mslo*), and *Drosophila* maxi K^+ channel α-subunit (*dslo*) (1, 5, 32). Proposed membrane-spanning segments are highlighted by a line below the sequences and designated as S1–S10. Two spliced sites are marked by arrows. *B*: differences between two isoforms, *rbslo1* and *rbslo2*.

replaced by perfusion. The oocytes were voltage clamped at −80 mV. Immediately after depolarization to +30 mV for 200 ms, the membrane potential was changed to the commanded voltage, from −80 mV to +40 mV.

Expression in Chinese hamster ovary cells. The *Sal* I-*Nde* I fragments of *rbslo* cDNA were treated with T4 DNA polymerase and blunt-end ligated into *Sal* I and *Xba* I-digested pGFP-N1 (Clontech). With these restriction enzymes, a fragment of cDNA coding GFP protein was cut out, and only *rbslo* cDNA remained in the constructs. The plasmid DNA was prepared separately with cesium trifluoroacetate centrifugation method. Chinese hamster ovary-K1 cells (CHO cells) were obtained from American Type Culture Collection (Rockville, MD) and grown on glass coverslips (Belleco Glass) in the following culture medium: 90% Ham's F-12 medium (Mediatech) and 10% fetal bovine serum (Hyclone). Calcium phosphate precipitation method was employed to transfect plasmids into CHO cells. To identify cells transiently transfected, an expression construct containing the murine T lymphocyte-specific surface protein, CD4, was used (12). Cells expressing

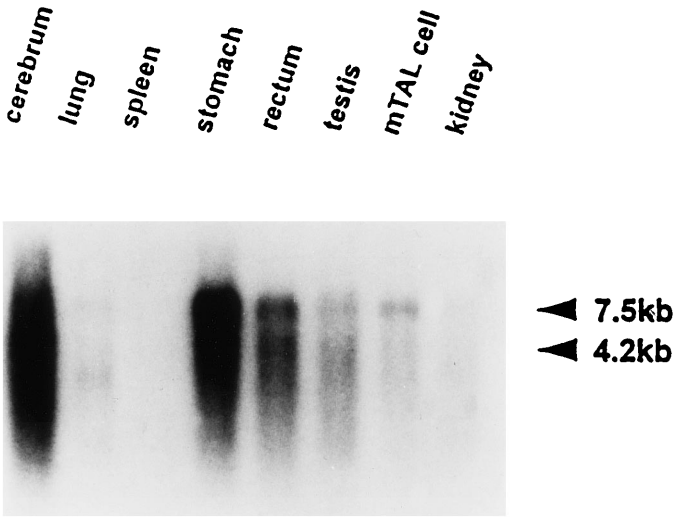

Fig. 3. Northern blot. Two micrograms of poly(A)+ RNA were loaded in each lane. A 4.1-kb *rbslo1* cDNA was random radiolabeled and used as probe. MTAL, medullary thick ascending limb.

CD4 were identified by attachment of CD4 antibody-coated beads (Dynail). On the 2nd and 3rd days after transfection only, cells with attached beads were chosen for whole cell and single-channel patch-clamp recordings (8). Command protocols were generated, and currents were acquired by using a List EPC-7 patch-clamp amplifier (Medical System) interfaced to a IBM-AT-compatible 486 microcomputer (Gateway 2000) via pCLAMP version 6.0.2 software (Axon Instruments). Data from single-channel recordings were low-pass filtered at 3 kHz and digitized at 12.5 kHz. For whole cell recordings, the pipette solution contained (in mM) 145 KCl, 5 NaCl, 1 $MgCl_2$, 10 HEPES, 118 $CaCl_2$, and 1 ethylene glycol-bis(β-aminoethyl ether)-*N*,*N*,*N*′,*N*′-tetraacetic acid (pH 7.4) [free Ca^{2+} is 10^{-8} M calculated using the program obtained from Dr. Marshall H. Montrose (Department of Medicine, The Johns Hopkins University)]. The bath solution contained (in mM) 145 KCl, 5 NaCl, 1 $MgCl_2$, 10 HEPES, and 1 $CaCl_2$ (pH 7.4) unless stated otherwise. For single-channel recordings (inside-out configuration), 150 mM KCl was used both in the pipette and bath solutions instead of a combination of 145 mM KCl and 5 mM NaCl. Free Ca^{2+} concentration in the bath solution was changed for checking Ca^{2+} sensitivity according to the program described above.

RESULTS

Primary structure of rbslo. Screening of MTAL cell cDNA library resulted in isolation of two sizes of cDNA fragments. Because both cDNA fragments did not contain 5′ end of cDNA, rapid amplification of cDNA ends-PCR was performed, and PCR products were ligated to the cDNA (Fig. 1). Nucleotide sequence comparison indicated that two cDNA fragments are quite homologous with each other; however, some differences were observed. The longer clone (*rbslo1*), encoding 1,215 amino acids, has a novel "in-frame" 174-bp insertion, which is located after the S8 transmembrane segment (splice *site A*). The shorter clone (*rbslo2*) encoding 796 amino acids has a 104-bp deletion between the predicted S9 and S10 segments (splice *site B*), creating a frame shift that introduced a premature termination codon at the 45 bp downstream of the deletion site. Only 16 amino acids encoded by *rbslo2* cDNA are different from *rbslo1* (amino acid similarity is 97.9%). The deduced amino acid sequences are shown in Fig. 2.

Rbslo1 has one potential adenosine 3′,5′-cyclic monophosphate/guanosine 3′,5′-cyclic monophosphate (cAMP/cGMP)-dependent protein kinase phosphorylation site, 15 protein kinase C phosphorylation sites, and 14 potential casein kinase II phosphorylation sites. *Rbslo2* has no cAMP/cGMP-dependent protein kinase phosphorylation site in the putative intracellular region but 10 potential protein kinase C phosphorylation sites and eight casein kinase II phosphorylation sites.

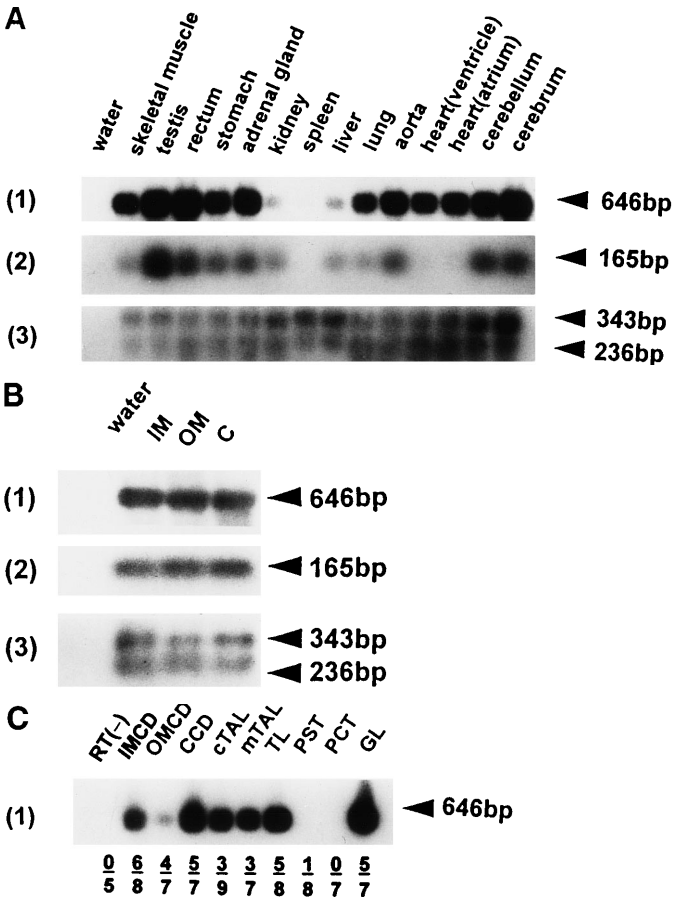

Fig. 4. *A*: PCR localization of *rbslo* among different tissues, *B*: 3 regions of rabbit kidneys, *C*: along nephron segments. Primers used for each PCR are indicated at *left* in parentheses. Sites of PCR primers used were shown in Fig. 1 and as follows: P region, S7 (*primer 1*); at splice *site A*, both primers are located in the additional exon in *rbslo1* (*primer 2*); at the splice *junction B*, both primers are upstream and downstream of deleted exon in *rbslo2* (*primer 3*). Predicted sizes of PCR products from *rbslo* clones are indicated at *right* (arrowheads): *primer 1*, 646-bp bands for both *rbslo1* and *rbslo2*; *primer 2*, 165 or (*primer 3*) 343-bp bands for *rbslo1*; *primer 3*, 236-bp bands for *rbslo2*. *C*: numbers at *bottom* indicate number of positive experiments (underlined) in total experiments for each nephron segment. *B*: IM, inner medulla; OM, outer medulla; C, cortex. *C*: RT(−), without reverse transcriptase; IMCD, inner medullary collecting duct; OMCD, outer medullary collecting duct; CCD, cortical collecting duct; CTAL, cortical thick ascending limb of Henle's loop; MTAL, medullary thick ascending limb of Henle's loop; TL, thin limbs of Henle's loop; PST, proximal straight tubule; PCT, proximal convoluted tubule; GL, glomerulus.

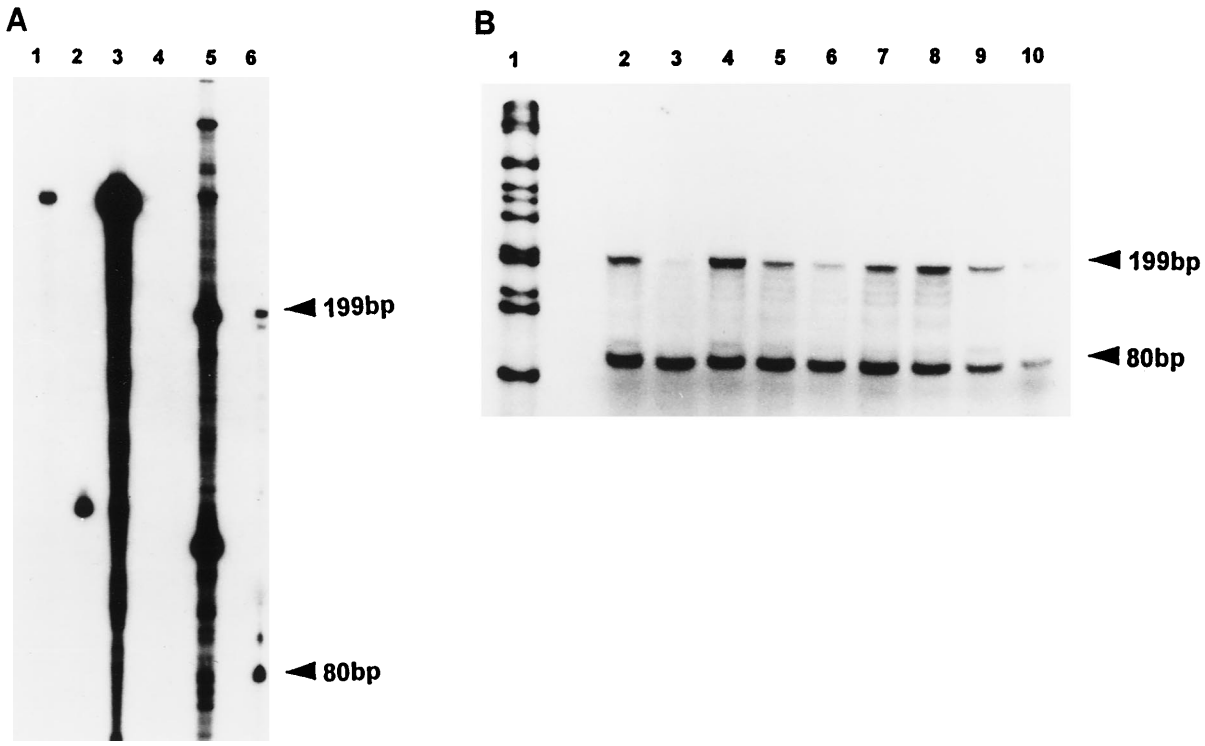

Fig. 5. Ribonuclease protection assay of *rbslo* expression. Site of probe was between S9 and S10 on cDNA sequence of *rbslo1*. Predicted sizes of protected fragments for *rbslo1* (199 bp) were detected. As internal control, 18S ribosomal RNA probe was added to each reaction and detected as 80-bp bands. Predicted bands for *rbslo2* were not observed here. *A*: *lane 1*, *rbslo* probe without hybridization; *lane 2*, 18S probe without hybridization; *lane 3*, both probes hybridized with yeast tRNA (2 μg) without treatment of ribonuclease; *lane 4*, both probes hybridized with yeast tRNA (2 μg) with treatment of ribonuclease; *lane 5*, RNA ladder; *lane 6*, both probes hybridized with MTAL cell total RNA (20 μg) with treatment of ribonuclease. *B*: total RNA used was as follows. *Lane 1*, 1-kb DNA ladder; *lanes 2* and *5*, 40 μg of total RNA from cortex; *lanes 3* and *6*, 40 μg of total RNA from outer medulla; *lanes 4* and *8*, 40 μg of total RNA from inner medulla; *lane 7*, 80 μg of cortex total RNA; *lane 9*, 20 μg of cortex total RNA; *lane 10*, 10 μg of cortex total RNA.

Tissue distribution of rbslo. Northern blot analysis revealed that *rbslo* mRNA is expressed in various rabbit tissues including MTAL cells, cerebrum, lung, stomach, rectum, and testis. Two different transcript sizes were detected (4.2 and 7.5 kb, Fig. 3). The signal in kidney is quite faint, suggesting a lower level of expression. RT-PCR was employed to distinguish the expression of isoforms as described in MATERIAL AND METHODS. Because the genomic sequence of this gene was not known, to eliminate the possibility of amplification of the genomic DNA, three sets of primers were used for RT-PCR. The primers were chosen empirically, such that the amplification from genomic DNA would result in different sizes of products from the amplification from cDNA. Control experiments also showed that no bands were observed in the absence of reverse transcriptase (data not shown).

Both PCR products amplified from *rbslo1* cDNA and *rbslo2* cDNA were detected in several tissues (Fig. 4; 646 bp bands for *rbslo1* and *rbslo2*, 165 bp or 343 bp bands for *rbslo1*, 236 bp bands for *rbslo2*), indicating that both isoforms are expressed widely throughout the body. In the kidney, both isoforms are expressed in cortex, outer medulla, and inner medulla (Fig. 4*B*). RT-PCR of microdissected nephron segments produced positive PCR products corresponding to *rbslo1* and *rbslo2* (646 bp) in glomeruli, thin limbs of Henle's loop, cortical and medullary ascending limbs of Henle's loop, cortical collecting tubules, and outer and inner medullary collecting ducts. Importantly, the predicted sizes of PCR products were hardly detected in proximal convoluted tubules (0 positive in $n = 7$) and proximal straight tubules (1 positive in $n = 8$) (Fig. 4*C*).

RPA indicated that the protected bands corresponding to *rbslo1* mRNA (199 bp) were observed in all regions of kidney, and the sequence of the abundance of *rbslo1* mRNA was as follows: inner medulla > cortex > outer medulla (Fig. 5). The predicted size of the protected bands (62 bp) for *rbslo2* were not consistently detected in the RPA.

Functional expression of rbslo in Xenopus oocyte and CHO-K1 cells. The individual cRNAs were prepared and injected into *Xenopus* oocytes separately as described in MATERIAL AND METHODS. Depolarization-activated outward currents were detected from *rbslo1* cRNA injected oocytes on the 2nd day after injection but not from *rbslo2* cRNA-injected oocytes. The *rbslo1* currents expressed in *Xenopus* oocytes are slightly inactivated with time and outwardly rectifying. Currents reach a 1 μA amplitude on the 2nd day, but, after the 3rd day, the oocytes could not be clamped to the command voltages because the expressed currents are

too large. The amplitude of the expressed currents decreased following application to the bath of either Ba^{2+} (5 mM), tetraethylammonium (TEA) (5 mM), or of IBTX (20 nM), a specific blocker of maxi K^+ channels (6) (Fig. 6). The ion selectivity of the expressed oocyte currents was measured by deactivation tail current experiments as described in MATERIAL AND METHODS. The reversal potential shifted from -29.7 ± 4.0 to -35.8 ± 7.4, -39.5 ± 9.6, and -52.2 ± 12.7 mV after 20 mM K^+ in the bath solution was replaced by Rb^+, NH_4^+, and Na^+, respectively ($n = 7$). These results suggested that the sequence of ion selectivity was $K^+ > Rb^+ > NH_4^+ > Na^+$.

On the 2nd–3rd days after *rbslo1* cDNA were transfected into CHO cells, currents were detected in both whole cell and inside-out single-channel configurations. Transfected CHO cells expressed large conductance, K^+-selective channels with properties characteristic of maxi K^+ channels (8, 15, 20, 21, 24), whereas nontransfected CHO cells and those transfected with vector alone did not show similar currents under the same experimental conditions. In the whole cell configuration, outward currents were observed with step depolarizations >0 mV. Ionomycin (1 μM), which increases intracellular Ca^{2+}, induced currents that are threefold at 100 mV (from 1,446 ± 272 to 5,010 ± 773 pA, $n = 10$) (Fig. 7*A*). *Rbslo1* currents showed little or no inactivation during the 350-ms voltage protocols. When the K^+ concentration ($[K^+]_o$) was changed in the extracellular solution, the extrapolated zero-current potential shifted from 0.1 ± 0.6 mV for 140 mM $[K^+]_o$ to -24.3 ± 1.8 mV for 50 mM $[K^+]_o$, -34.2 ± 2.0 mV for 24.3 mM $[K^+]_o$, and -51.5 ± 1.6 mV for 10 mM $[K^+]_o$. During changes in the extracellular solution, $[K^+]_i$ was kept 140 mM, resulting in an Na^+-to-K^+ permeability ratio = 0.04 (Fig. 7*B*). *Rbslo1* currents were blocked by external TEA (5 mM) and IBTX (20 nM) (data not shown). Single-channel amplitude varied linearly with voltage in symmetrical K^+ concentrations ($[K^+]$ = 150 mM) with a slope conductance of 245.3 ± 2.6 pS and a reversal potential of 0.03 ± 0.80 mV ($n = 7$, Fig. 8*A*). Open channel probability increased when the intracellular side of a single patch was exposed to 0.1 μM Ca^{2+} and voltage was changed over the range of −70 mV to +70 mV (Fig. 8*A*). The probability of the channel being open at a given voltage was dependent on the $[Ca^{2+}]_i$ (Fig. 8, *B* and *C*). Thus *rbslo1* channel is both voltage and Ca^{2+} dependent.

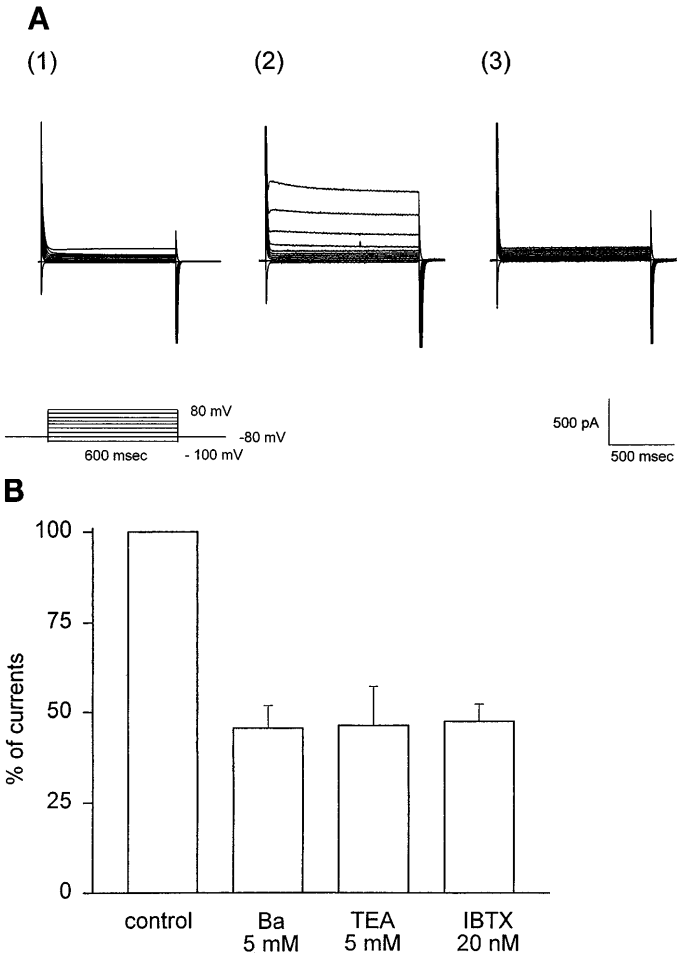

Fig. 6. Expression of *rbslo1* in *Xenopus* oocytes. Two-electrode voltage clamping was performed in ND96 solution with 150 μM niflumic acid. Oocytes were clamped at −80 mV, and voltage steps were from −100 mV to +80 mV in 20-mV increments, 600 ms in duration. *A*: current traces from oocytes injected with H_2O (*A1*) or *rbslo1* cRNA (*A2* and *A3*). Outward currents detected in cRNA injected oocytes (*A2*) were blocked after an addition of 5 mM tetraethylammonium (TEA) to the bath (*A3*). *B*: blockade of expressed currents by application of TEA (5 mM), Ba^{2+} (5 mM), or iberiotoxin (IBTX, 20 nM) to the bath. Amplitude of expressed currents decreased following application of either Ba^{2+} (5 mM) or TEA (5 mM) to the bath (45.5 ± 3.1%, $n = 4$; 46.3 ± 9.0%, $n = 3$, respectively, in current amplitude at +80 mV compared with that before application). Addition of IBTX (20 nM) to bath inhibited expressed currents in 10 min (35.5 ± 10.2%, $n = 4$). Results are expressed as percentage of currents before application of reagents, and data are means ± SE.

DISCUSSION

Primary structure of maxi K^+ channels and functional expression. We have cloned two alternative transcripts, *rbslo1* and *rbslo2*, of the maxi K^+ channel with novel sequences. *Rbslo1* has a novel insert of 59 novel amino acids at splice *site A*. *Rbslo2* has a portion missing at splice *site B*, which creates a frame shift, causing truncation of the COOH terminus (Fig. 2). The overall amino acid identity of *rbslo1* to mouse, *mslo*, and to *Drosophila* (*dslo*) α-subunits is very high (Fig. 1). Also, between the mammalian *rbslo* clones, amino acid sequences are well conserved, including the alternative splicing *site A*. On the other hand, the splice *site B* in *rbslo2* is novel (Fig. 2). Several alternate transcripts of maxi K^+ channel α-subunits have been reported from different species (14, 32). For example, four splice variants were reported in the human α-subunit (*hslo*) derived from human brain cDNA library (32). These variants occur at splice *site 2* of *hslo* that corresponds to splice *site A* of *rbslo1*. However, none of the *hslo* variants includes an insertion of a novel exon. At splice *site B* of *rbslo2*, there have been no previous reports concerning splice variants of the α-subunit that create a frame shift and a truncation of the COOH terminus.

Electrophysiological characterization of rbslo1 and rbslo2. We have used two expression systems (*Xenopus* oocytes and CHO cells) to characterize the channels. Voltage-activated, iberiotoxin-sensitive, Ca^{2+}-sensitive, outward K^+ currents were detected only from the oocytes or CHO cells in which *rbslo1* cRNA was expressed (Fig. 6). No currents were observed from *rbslo2* expressed in *Xenopus* oocytes. *Rbslo1* channel could be characterized as a maxi Ca^{2+}-activated K^+ channel by the following characteristics: *1*) single-channel conductance of 245 pS in symmetrical 150 mM KCl solutions, *2*) high-K^+ selectivity over Na^+ (Na^+-to-K^+ permeability ratio = 0.04) and ion selectivity sequence of $K^+ > Rb^+ > NH_4^+ > Na^+$, *3*) left shift of the voltage-open probability relationship of the expressed channels at increasing intracellular calcium concentration, *4*) outwardly rectifying voltage-dependent currents with little or no inactivation in voltage clamping and whole cell current recording, and *5*) the expressed currents are sensitive to iberiotoxin. Some of these characteristics were common among the expressed channels previously reported as *slo* maxi K^+ channel α-subunits (1, 5, 18, 32).

The unique feature of *rbslo1* is greatly enhanced Ca^{2+} and voltage sensitivities compared with previously cloned α-subunits. For example, the membrane potential to achieve a half-maximal conductance ($V_{½}$) for *rbslo1* expressed in CHO cells is 61 mV at 0.1 μM Ca^{2+} and −33 mV at 1 μM Ca^{2+} at symmetrical 150 mM [K^+]. In comparison, for the *hslo* channel (hbr5), $V_{½}$ at 2.4 μM $[Ca^{2+}]_i$ with symmetrical 110 mM [K^+] is ~0 mV (32), much more positive than what we observed for the *rbslo1* channel. For the *mslo* channel (mbr5), the $V_{½}$ at 10 μM $[Ca^{2+}]_i$ with symmetrical 156 mM [K^+] is +23.4 mV (5). The *mslo* channel (mbr5) has a very low open probability at voltages more negative than +60 mV when $[Ca^{2+}]_i$ was 1 μM, whereas, for *rbslo1*, the open probability is very high at the same conditions. Thus *rbslo1* is at least an order of magnitude more sensitive.

Coexpression studies of the α-subunit of Ca^{2+}-activated K^+ channels with the α-subunit produces maxi K^+ channels with greater Ca^{2+} and voltage sensitivities than when the α-subunit is expressed alone (11, 19). Thus the α-subunit seems to act as a modulator of channel activity. In our studies, we observed that a unique feature of *rbslo1* is a relatively high Ca^{2+} sensitivity when expressed in CHO cells in the absence of the α-subunit. One possibility is that CHO express the α-subunit endogenously. However, others have provided evidence (18) implying that the α-subunit is not expressed endogenously in CHO cells. To test this directly, we used degenerate PCR primers that could successfully amplify rabbit maxi K^+ channel α-subunit

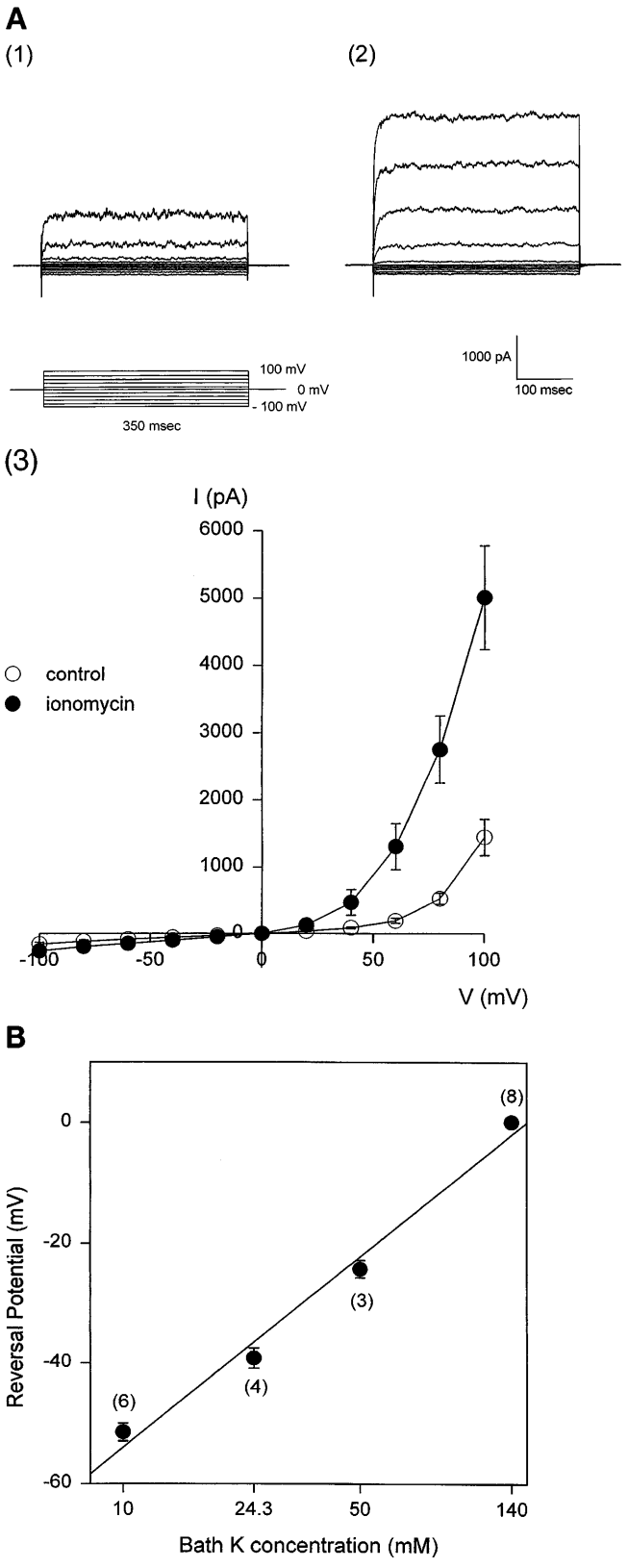

Fig. 7. *Rbslo1* currents detected by whole cell clamping of transduced CHO cells. Whole cell currents were Ca^{2+} activated and K^+ selective. *A*: representative traces before (*A1*) and after (*A2*) application of ionomycin (1 μM). *A3*: current-voltage relationship for *rbslo1*. Holding potential was 0 mV, followed by 350-ms step voltage pulse from −100 mV to +100 mV by 20-mV increments. *B*: relationship between reversal potential and extracellular K^+ concentration. Deactivation tail current experiments were performed. K^+ concentration was altered by replacing NaCl with KCl in bath solutions. Permeability ratio was calculated from the Goldman-Hodgkin-Katz equation. Voltage protocol was −80 mV holding potential, depolarized to +100 mV, 400 ms, then step voltage from −140 mV to +100 mV in 20-mV increments, 500 ms in duration. Data are means ± SE. Number of experiments are given in parentheses.

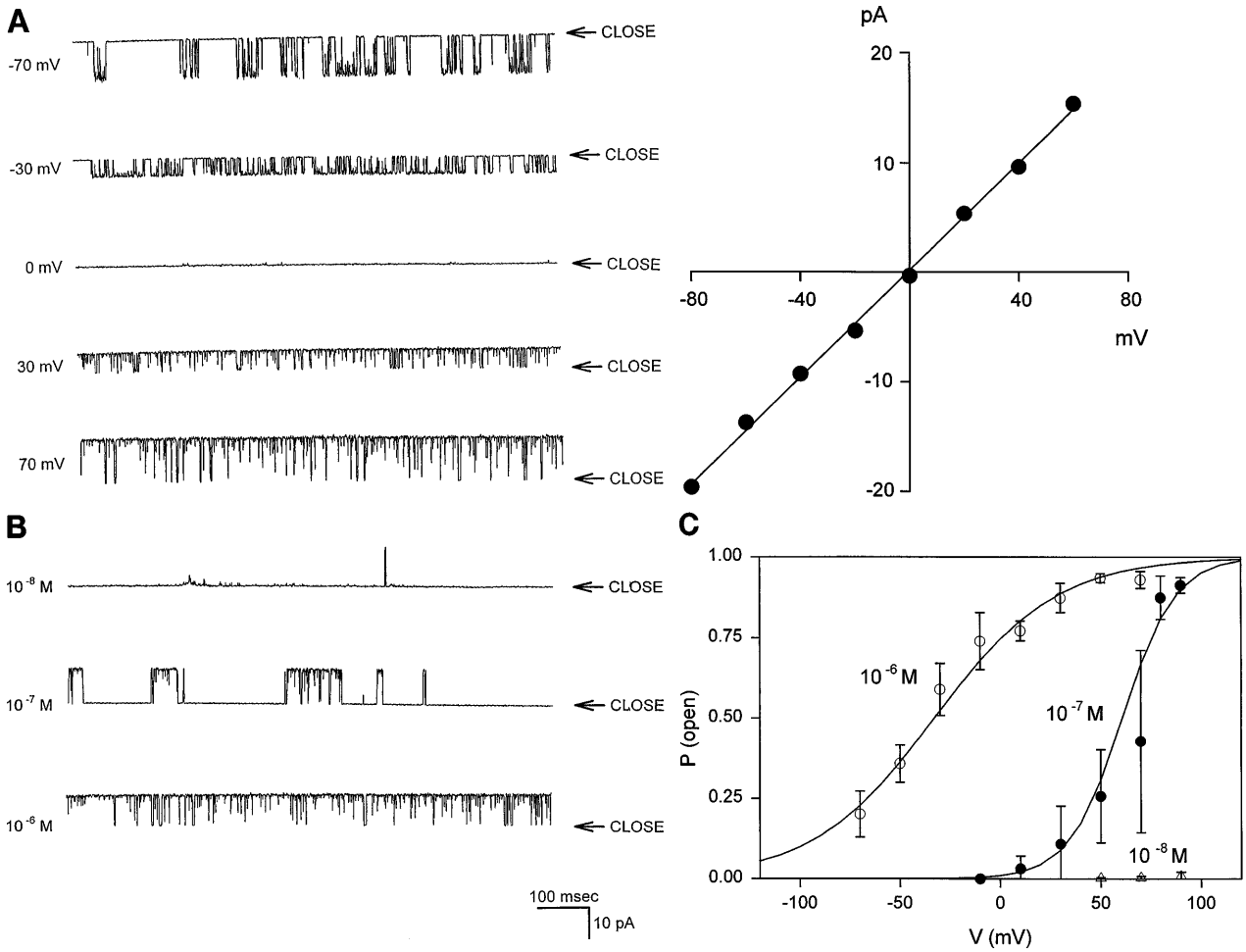

Fig. 8. *Rbslo1* channels detected by inside-out patch clamping in transfected CHO cells. *A*, *left*: records of *rbslo1* channel activity at different voltages. Closed states are indicated by arrows. $[Ca^{2+}]_i$ was 1 μM. K^+ concentration on both sides of the membrane was 150 mM. *A*, *right*: current-voltage relations for *rbslo1* in inside-out configuration. *B*: records of *rbslo1* channel activity in different Ca^{2+} concentrations (at +50 mV). $[Ca^{2+}]_i$ is indicated at *left* of each trace. *C*: open probabilities (P_{open}) at different $[Ca^{2+}]_i$ and voltages (*V*). $[Ca^{2+}]_i$ values are indicated near traces. Data are means ± SE (each $n = 3$). Data were collected from observations on a patch containing only one active channel, and the continuous lines were optimized fits to the Boltzmann function.

but could not observe the predicted size of PCR product for maxi K^+ channel α-subunit in the cDNA from CHO cells (data not shown). Thus enhanced sensitivity is most likely an intrinsic property of *rbslo1* independent of the α-subunit.

In the *Drosophila* α-subunit, three variable splicing regions after S6 segment were found to be responsible for the functional differences, such as Ca^{2+} sensitivity, unit conductance, and gating kinetics (14). Given the high homology of *rbslo1* to *dslo*, except for the novel *rbslo1* sequence at *site A*, it is likely that this novel exon might be responsible for the different Ca^{2+} sensitivity of *rbslo1* maxi K^+ channels. However, further mutagenesis studies will be needed to prove this point conclusively.

Although we could not detect voltage-activated outward currents from the oocytes in which *rbslo2* cRNA was injected, this transcript might be involved in the modification of Ca^{2+}-activated K^+ current through coassembly with other spliced variants or the regulation of mRNA through splicing mechanisms (14). Coexpression of *rbslo1* cRNA and *rbslo2* cRNA in *Xenopus* oocytes indicated a decrease of current amplitude compared with the expression of *rbslo1* cRNA alone (data not shown).

Wei et al. (33) showed that the second half (from splice *site A* to COOH terminus) of maxi K^+ channel α-subunit is essential for its calcium and voltage sensitivity. Considering that channel activity was not observed in *rbslo2*-injected *Xenopus* oocytes, it may be possible that the region after S9 segment is necessary to function as a Ca^{2+}-activated K^+ channel. Further study including detection of protein expression is required to answer this question.

Intrarenal distribution of maxi K+ channel α-subunit. Maxi K^+ channel activity assessed by the patch-clamp technique has been detected throughout the kidney in mesangial (24), proximal tubule (10, 20), medullary and cortical thick ascending limb (8, 21), and principal (15) and intercalated cells (23) in the cortical collecting duct. Our experiments have detected *rbslo* transcripts in the same nephron segments where maxi

K^+ channel activity was detected by electrophysiological methods. This confirms conclusively that maxi K^+ channels are expressed in multiple nephron segments of rabbit kidney.

Interestingly, it is difficult to detect expression in proximal tubules, especially in the convoluted segment. Among all of the previous electrophysiological studies, there is no report that directly demonstrates the existence of channels with properties identical to maxi K^+ channels in intact mammalian proximal tubules. Zweifach et al. (34) detected large-conductance K^+ channels by fusing the apical membrane of membrane vesicles from proximal to planar lipid bilayers. However, the single-channel conductance and voltage dependence of the channels were substantially different from those of maxi K^+ channels detected using apical membranes of distal nephron. Likewise, Tauc et al. (30) found that the sensitivity of maxi K^+ channels to iberiotoxin in primary cultured proximal collecting tubule cells was much lower than that of the maxi K^+ channels present in smooth muscle cells (30). Iberiotoxin is thought to inhibit maxi K^+ channels by blocking their channel pores from the extracellular side (6). Thus a different iberiotoxin sensitivity of maxi K^+ channels in proximal cells from intact tubules combined with our inability to detect the predicted bands amplified from *rbslo* by RT-PCR in freshly dissected tubules may suggest that different functional maxi K^+ channel subunits are expressed in proximal tubule segments. It should be mentioned that, Kawahara et al. (10) did demonstrate that hypotonicity (218 mosmol/kgH_2O) activated typical maxi-type K^+ channels in rabbit PCT primary cultured cells. However, it is possible that cells in culture may have a different pattern of channel expression than intact tubule cells, as was reported for delayed-rectifier, voltage-gated K^+ channels (7). Another type of Ca^{2+}-activated K^+ channel, which has a single transmembrane domain, is expressed abundantly in proximal tubules (4, 26, 27). This channel, which is activated both by hypotonicity and depolarization produces a slowly activating current when the cRNA is injected *Xenopus* oocytes. It is possible that this channel is responsible for Ca^{2+}-activated K^+ currents in the native proximal tubule.

Our RPA indicated that the order of *rbslo1* mRNA abundance is inner medulla > cortex > outer medulla. We could not consistently detect protected bands corresponding to *rbslo2* mRNA by RPA, probably because of low abundance of *rbslo2* mRNA. The expected size of PCR products for *rbslo2* mRNA was detected by RT-PCR (Fig. 4). In addition to the two splice variants of *rbslo* isolated from MTAL cells, it is still possible that other splice variants may exist in the kidney, which were not identified in this study. Rare isoforms might not be amplified sufficiently to be detected.

In conclusion, maxi K^+ channels are thought to play an important role in regulatory volume decrease. Our data show that *rbslo* maxi K^+ channels are expressed most abundantly in inner medulla. Given that the inner medulla is subjected to large changes in osmolality during different diuretic states, it is possible that Ca^{2+}-activated K^+ channels may have a role in volume regulation in this portion of the kidney.

We thank Dr. Min Li (Dept. of Physiology, The Johns Hopkins University) for kindly providing CD4 plasmid.

This work was funded by National Institute of Diabetes and Digestive and Kidney Diseases Grant DK-32753.

Address for reprint requests: W. B. Guggino, Dept. of Physiology, School of Medicine, The Johns Hopkins Univ., 725 N. Wolfe St., Baltimore, MD 21205.

Received 29 January 1997; accepted in final form 15 May 1997.

REFERENCES

1. **Adelman, J. P., K. Shen, M. P. Kavanaugh, R. A. Warren, Y. Wu, A. Lagrutta, C. T. Bond, and R. A. North.** Calcium-activated potassium channels expressed from cloned complementary DNAs. *Neuron* 9: 209–216, 1992.
2. **Alioua, A., J. P. Huggins, and E. Rousseau.** PKG-Iα phosphorylates the α-subunit and upregulates reconstituted GK_{Ca} channels from tracheal smooth muscle. *Am. J. Physiol.* 268 (*Lung Cell. Mol. Physiol.* 12): L1057–L1063, 1995.
3. **Berg, M., N. Green, S. R. Steel, and J. Handler.** Differentiated function in cultured epithelia derived from thick ascending limbs. *Am. J. Physiol.* 242 (*Cell Physiol.* 11): C229–C233, 1982.
4. **Busch, A. E., and F. Lang.** Effect of $[Ca^{2+}]_i$ and temperature on min K channels expressed in Xenopus oocytes. *FEBS Lett.* 334: 221–224, 1993.
5. **Butler, A., S. Tsunoda, D. P. McCobb, A. Wei, and L. Sarkoff.** *Mslo*, a complex mouse gene encoding "maxi" calcium-activated potassium channels. *Science* 261: 221–224, 1993.
6. **Candia, S., M. L. Garcia, and R. Latorre.** Mode of action of iberiotoxin, a potent blocker of the large conductance Ca^{2+}-activated K^+ channel. *Biophys. J.* 63: 583–590, 1992.
7. **Doerner, D., T. A. Pitler, and B. E. Alger.** Protein kinase C activators block specific calcium and potassium current components in isolated hippocampal neurons. *J. Neurosci.* 8: 4069–4078, 1988.
8. **Guggino, S. E., W. B. Guggino, N. Green, and B. Sacktor.** Ca^{2+}-activated K^+ channels in cultured medullary thick ascending limb cells. *Am. J. Physiol.* 252 (*Renal Fluid Electrolyte Physiol.* 21): C121–C127, 1987.
9. **Guggino, S. E., W. B. Guggino, and B. Sacktor.** Forskolin and antidiuretic hormone stimulate a Ca^{2+}-activated K^+ channel in cultured kidney cells. *Am. J. Physiol.* 249 (*Renal Fluid Electrolyte Physiol.* 18): F448–F455, 1985.
10. **Kawahara, K., A. Ogawa, and M. Suzuki.** Hypotonic activation of Ca-activated K channels in cultured rabbit kidney proximal tubular cells. *Am. J. Physiol.* 260 (*Renal Fluid Electrolyte Physiol.* 29): F27–F33, 1991.
11. **Knaus, H. G., K. Folander, M. Garcia-Calvo, M. L. Garcia, G. J. Kaczorowski, M. Smith, and R. Swanson.** Primary sequence and immunological characterization of α-subunit of high conductance Ca^{2+}-activated K^+ channel from smooth muscle. *J. Biol. Chem.* 269: 17274–17278, 1994.
12. **Krapivinsky, G., E. A. Gordon, K. Wickman, B. Velimirovic, L. Krapivinsky, and D. E. Clapham.** The G-protein-gated atrial K^+ channel IKACh is a heteromultimer of two inwardly rectifying K^+-channel proteins. *Nature* 374: 135–141, 1995.
13. **Kume, H., A. Takai, H. Tokuno, and T. Tomita.** Regulation of Ca^{2+}-dependent K^+ channel activity in tracheal myocytes by phosphorylation. *Nature* 341: 152–154, 1989.
14. **Lagrutta, A., K. Shen, A. North, and J. P. Adelman.** Functional differences among alternatively spliced variants of slopoke, a *Drosophila* calcium-activated potassium channel. *J. Biol. Chem.* 269: 20347–20351, 1994.
15. **Ling, B. N., C. F. Hinton, and D. C. Eaton.** Potassium permeable channels in primary culture of rabbit cortical collecting tubule. *Kidney Int.* 40: 441–452, 1991.
16. **Lu, L., C. Montrose-Rafizadeh, and W. B. Guggino.** Ca^{2+}-activated K^+ channels from rabbit kidney medullary thick ascending limb cells expressed in *Xenopus* oocytes. *J. Biol. Chem.* 265: 16190–16194, 1990.
17. **McCarty, N. A., and R. G. O'Neil.** Calcium-dependent control of volume regulation in renal proximal tubule cells. II. Roles of

dihydropyridine-sensitive and -insensitive Ca^{2+} entry pathway. *J. Membr. Biol*. 123: 161–170, 1991.

18. **McCobb, D. P., N. L. Fowler, T. Featherstone, C. J. Lingle, M. Saito, J. E. Krause, and L. Salkoff.** A human calcium-activated potassium channel gene expressed in vascular smooth muscle. *Am. J. Physiol*. 269 (*Heart Circ. Physiol*. 38): H767–H777, 1995.
19. **McManus, D. B., L. M. H. Heins, L. Pallanck, B. Ganetzky, R. Swanson, and R. J. Leonard.** Functional role of the α-subunit of high conductance calcium-activated potassium channels. *Neuron* 14: 645–650, 1995.
20. **Merot, J., M. Bidet, S. L. Maout, M. Tauc, and P. Pojeol.** Two type of K^+ channels in the apical membrane of rabbit proximal tubule in primary culture. *Biochim. Biophys. Acta* 978: 134–144, 1989.
21. **Merot, J., V. Poncet, M. Bidet, M. Tauc, and P. Poujeol.** Apical membrane ionic channels in the rabbit cortical thick ascending limb in primary culture. *Biochim. Biophys. Acta* 1070: 387–400, 1991.
22. **Montrose-Rafizadeh, C., and W. B. Guggino.** Role of intracellular calcium in volume regulation by medullary thick asecending limb cells. *Am. J. Physiol*. 260 (*Renal Fluid Electrolyte Physiol*. 29): F402–F409, 1991.
23. **Pacha, J., G. Frindt, H. Sackin, and L. G. Parmer.** Apical maxi K channels in intercalated cells in CCT. *Am. J. Physiol*. 261 (*Renal Fluid Electrolyte Physiol*. 30): F696–F705, 1991.
24. **Stockand, J. D., and S. C. Sansom.** Large Ca^{2+}-activated K^+ channels responsive to angiotensin II in cultured human mesangial cells. *Am. J. Physiol*. 267 (*Cell Physiol*. 36): C1080–C1086, 1994.
25. **Stoner, L. C., and G. E. Morley.** Effect of basolateral or apical hyposmolarity on apical maxi K channels of everted rat collecting tubule. *Am. J. Physiol*. 268 (*Renal Fluid Electrolyte Physiol*. 37): F569–F580, 1995.
26. **Sugimoto, T., Y. Tanabe, R. Shigemoto, M. Iwai, T. Takumi, H. Ohkubo, and S. Nakanishi.** Immunological study of a rat membrane protein which induces a selective potassium permeation: its localization in the apical membrane portion of epithelial cells. *J. Membr. Biol*. 113: 39–47, 1990.
27. **Takumi, T., H. Ohkubo, and S. Nakanishi.** Cloning of a membrane protein that induces a slow voltage-gated potassium current. *Science* 242: 1042–1045, 1988.
28. **Taniguchi, J., and W. B. Guggino.** Membrane stretch: a physiological stimulator of Ca^{2+}-activated K^+ channels in thick ascending limb. *Am. J. Physiol*. 257 (*Renal Fluid Electrolyte Physiol*. 26): F347–F352, 1989.
29. **Taniguchi, J., K. Furukawa, and M. Shigekawa.** Maxi K^+ channels are stimulated by cyclic guanosine monophosphate-dependent protein kinase in canine coronary artery smooth muscle cells. *Pflügers Arch*. 423: 167–172, 1993.
30. **Tauc, M., P. Congar, V. Poncet, J. Merot, C. Vita, and P. Poujeol.** Toxin pharmacology of the large-conductance Ca^{2+}-activated K^+ channel in the apical membrane of rabbit proximal convoluted tubule in primary culture. *Pflügers Arch*. 425: 126–133, 1993.
31. **Terada, Y., T. Moriyama, B. M. Martin, M. A. Knepper, and A. Garcia-Perez.** RT-PCR microlocalization of mRNA for guanylyl cyclase-coupled ANF receptor in rat kidney. *Am. J. Physiol*. 261 (*Renal Fluid Electrolyte Physiol*. 30): F1080–F1087, 1991.
32. **Tseng-Crank, J., C. D. Foster, J. D. Kraus, R. Metz, N. Godict, T. J. Dichiara, and P. H. Reinhart.** Cloning, expression, and distribution of functionally distinct Ca^{2+}-activated K^+ channel isoforms from human brain. *Neuron* 13: 1315–1330, 1994.
33. **Wei, A., C. Solaro, C. Lingle, and L. Sarkoff.** Calcium sensitivity of BK-type KCa channels determined by a separable domain. *Neuron* 13: 671–681, 1994.
34. **Zweifach, A., G. V. Desir, P. S. Aronson, and G. H. Giebisch.** A Ca-activated K channel from rabbit renal brush-border membrane vesicles in planar lipid bilayers. *Am. J. Physiol*. 261 (*Renal Fluid Electrolyte Physiol*. 30): F187–F196, 1991.